Salinosporamides D−J from the Marine Actinomycete *Salinispora tropica*, Bromosalinosporamide, and Thioester Derivatives Are Potent Inhibitors of the 20S Proteasome

Katherine A. Reed, Rama Rao Manam, Scott S. Mitchell, Jianlin Xu, Sy Teisan, Ta-Hsiang Chao, Gordafaried Deyanat-Yazdi, Saskia T. C. Neuteboom, Kin S. Lam, and Barbara C. M. Potts*

Nereus Pharmaceuticals, Inc., 10480 Wateridge Circle, San Diego, California 92121

Received July 17, 2006

Salinosporamide A (NPI-0052; **3**), a highly potent inhibitor of the 20S proteasome, is currently in phase I clinical trials for the treatment of cancer. During the course of purifying multigram quantities of **3** from *Salinispora tropica* fermentation extracts, several new salinosporamides were isolated and characterized, most of which represent modifications to the chloroethyl substituent at C-2. Specifically, **3** was isolated along with the known compound salinosporamide B (**4**), the previously undescribed methyl congener salinosporamide D (**7**), and C-2 epimers of **3** and **7** (salinosporamides F (**9**) and G (**10**), respectively). Salinosporamide I (**13**), in which the methyl group at the ring junction is replaced with an ethyl group, and the C-5 deshydroxyl analogue salinosporamide J (**14**), were also identified. Replacement of synthetic sea salt with sodium bromide in the fermentation media produced bromosalinosporamide (**12**), **4**, and its C-2 epimer (**11**, salinosporamide H). In addition to these eight new salinosporamides, several thioester derivatives were generated semisynthetically. IC_{50} values for cytotoxicity against human multiple myeloma cell line RPMI 8226 and inhibition of the chymotrypsin-like (CT-L) activity of purified rabbit 20S proteasomes were determined for all compounds. The results indicate that thioesters may directly inhibit the proteasome, albeit with reduced potency compared to their β-lactone counterparts.

Microorganisms have produced some of the most important inhibitors of the 20S proteasome, a multi-subunit enzyme complex that provides the primary pathway for degradation of ubiquitin-tagged proteins in eukaryotic cells. These natural product inhibitors offer potential new therapies for the treatment of multiple myeloma and other diseases[1] and have played a critical role in understanding proteasome structural biology by virtue of their unique binding mechanisms.[2] Proteasome inhibitors derived from microorganisms include TMC-95A and -95B from *Apiospora montagnei* Sacc. TC 1093,[3] belactosins from *Streptomyces* sp.,[4] and epoxomicin from actinomycete strain Q996-17,[5] along with a growing family of γ-lactam-β-lactone inhibitors. The first reported compound in this class was omuralide (*clasto*-lactacystin-β-lactone, **1**),[6] which is derived from lactacystin (**2**), a product of a *Streptomyces* strain.[7,8] Salinosporamide A[9] (NPI-0052; **3**) and its deschloro analogue salinosporamide B (**4**)[10] are uniquely derived from the marine actinomycete *Salinispora tropica*,[9,11] while several structurally related compounds (exemplified by **5**) have been isolated from terrestrial *Streptomyces* strain JS360.[12] The compounds in this growing family of γ-lactam-β-lactone inhibitors are distinguished by the substitution patterns about the bicyclic ring system. Specifically, **1** bears an isopropyl group at C-5 and a proton at the C-3 ring juncture, while **3**, **4**, and **5** bear cyclohexenyl and methyl groups at these respective positions. The secondary alcohol (*R*)-C-5OH is common across the series, with the exception of a single report of a C-5H_2 analogue of **5**.[12] The identity of the C-2 substituent varies from methyl (**1**)[6] to ethyl (**4**),[10] *n*-hexyl (**5**) or substituted *n*-hexyl,[12] and chloroethyl (**3**)[9] and imparts unique biological activity to molecules across the family, as indicated by SAR studies[13] and X-ray crystallographic analysis of **1**, **3**, and **4** in complex with the yeast 20S proteasome.[14] Interestingly, omuralide (**1**) is found in nature as its thioester precursor **2**, and thioesters of the subfamily of compounds represented by **5** have also been identified (e.g., **6**),[12] while no thioester analogues of salinosporamides have been reported to date. Detailed studies of β-lactone **1** and thioester **2** indicate that the β-lactone represents the species that enters the cell and reacts with the proteasome,[15,16] and in the case of **1**, **3**, and **4**, X-ray crystallographic studies have demonstrated that the catalytic N-terminal threonine residue of the proteasome is acylated by the β-lactone ring.[14,17]

During the course of large-scale fermentation and purification of **3** to support preclinical development and clinical trials, we isolated and characterized several new structurally related compounds, which provided an opportunity to further evaluate the structural diversity and biological activities of γ-lactam-β-lactone proteasome inhibitors derived from *S. tropica*. Additional analogues were obtained through modified fermentation conditions directed toward introducing bromine in place of chlorine.[18] Despite thorough examination of extracts, no thioester analogues of the salinosporamides were identified. We therefore generated a series of thioesters through derivatization of **3** and **4**. We report herein on the structures of these new analogues, their ability to inhibit the CT-L activity of the rabbit 20S proteasome, and their cytotoxicity against human multiple myeloma cell line RPMI 8226.

Results and Discussion

Isolation and Structure Elucidation of Salinosporamides D−J (7−14) and Bromosalinosporamide. Crude extracts generated from saline fermentation of *S. tropica* strain NPS000465 were subjected to normal-phase flash chromatography on Si gel, generating fractions enriched in the salinosporamides. Normal-phase HPLC was then utilized to separate **3** from its analogues, which were further purified using either reversed- or normal-phase HPLC. Most of the analogues represent modifications to the C-2 substituent, including salinosporamide D (**7**, R = methyl), the previously described salinosporamide B[10] (**4**, R = ethyl), and salinosporamide E (**8**, R = propyl). Stereoisomers included salinosporamide F (**9**), the C-2 epimer of **3**, and salinosporamide G (**10**), the C-2 epimer of **7**. In addition to these congeners, the crude extract also contained salinosporamide I (**13**), in which the methyl group at the ring junction is replaced with an ethyl group, as well as salinosporamide J (**14**), in which C-5 is dehydroxylated. A modified batch of crude extract was generated using fermentation conditions that incorporated a stepwise NaBr-enrichment scheme. These modified fermentation conditions produced **4** and its C-2 epimer salinosporamide H (**11**), along with **3** and the target brominated analogue **12**. Normal-phase flash chromatography on Si gel followed by reversed-

* To whom correspondence should be addressed. Phone: 858-200-8324. Fax: 858-587-4088. E-mail: bpotts@nereuspharm.com.

10.1021/np0603471 CCC: $37.00
Published on Web 01/23/2007

Chart 1

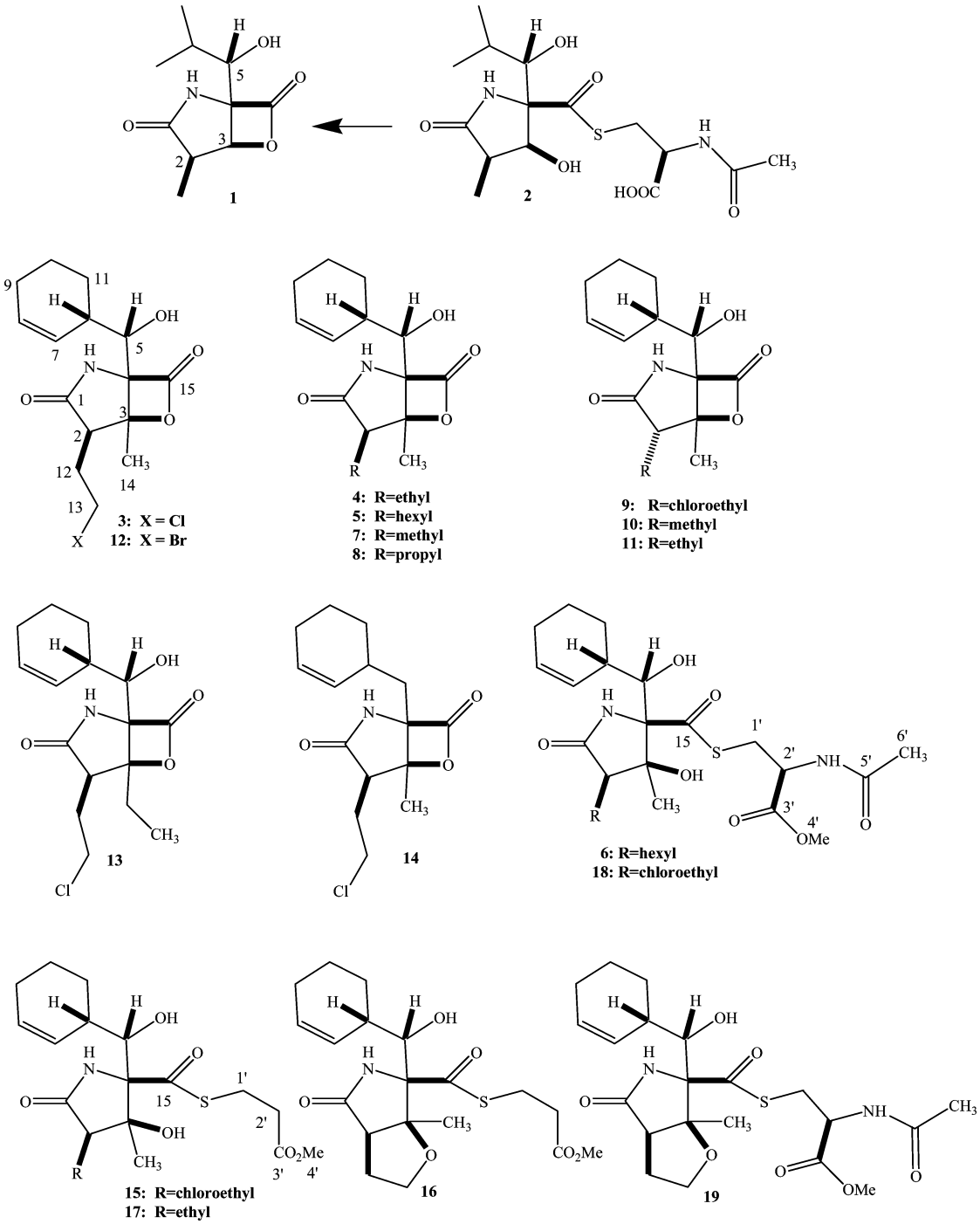

phase HPLC was used to separate compounds **3** and **4** from minor analogues **11** and **12**, which were further purified by normal-phase HPLC as necessary. The structures of these compounds have been determined by analysis of complete spectroscopic data, as described herein. NMR resonance assignments for all analogues were made through analysis of one- and two-dimensional NMR spectra, including COSY, multiplicity-edited HSQC, and HMBC experiments. The resulting ^{1}H and ^{13}C NMR assignments for **3** and its analogues are summarized in Tables 1 and 2. With respect to stereochemistry, the absolute configuration of **9** was determined by X-ray crystallography. For the remaining compounds, stereochemical assignments were made by analysis of NOE correlations and proton−proton coupling constants, together with diagnostic ^{1}H and ^{13}C chemical shifts established for 2*R* versus 2*S* salinosporamides (*vide infra*).

The series of analogues with *R* configuration at C-2 was characterized as follows. The structures of salinosporamides A (**3**) and B (**4**) were confirmed by comparison with authentic standards and published data.[9] The HRESIMS measurement for salinosporamide D (**7**, R = methyl; *m*/*z* 266.1396 $[M + H]^+$, Δ_{calc}= 1.2 ppm) indicated a molecular formula of $C_{14}H_{19}NO_4$, consistent with a molecule containing one less methylene group than **4**. The ^{1}H NMR spectrum of **7** contained a doublet methyl group at 1.06 ppm in place of the ethyl protons present in the ^{1}H NMR spectrum of **4**, establishing that **7** bears a methyl group at C-2. Analysis of 2-D spectroscopic data, including COSY, HSQC, and HMBC, provided additional support for the assignment of the structure. The relative stereochemistry for the three substituents about the bicyclic ring system was supported by strong NOESY correlations from H_3-14 to H-5 and H-2 but only a weak correlation from H_3-14 to H_2-12. Furthermore, the H-5/H-6 coupling constant compared favorably with that of **3** and **4** (Table 1). Collectively, these data support the

Table 1. ^{1}H NMR Assignments for Compounds **3**, **4**, and **7**−**14** (DMSO-d_6)[a,b]

position	3	4	7	8	9	10	11	12	13	14
2	2.65, t (7.0)	2.37, dd (8.2, 6.0)	2.52, q (7.4)	2.42, m	2.67, dd (9.7, 5.5)	2.56, q (7.7)	2.37, dd (7.9, 6.5)	2.64, t (7.0)	2.71, dd (9.1, 4.1)	2.80, t (6.9)
5	3.68, t (8.5)	3.65, t (8.2)	3.66, dd (9.1, 8.0)	3.66, t (8.5)	3.59, t (9.1)	3.58, t (8.9)	3.58, dd (8.9, 8.3)	3.67, dd (9.2, 8.0)	3.65, t (8.2)	1.82[a], m
6	2.28, m	2.28, m	2.27, m	2.28, m	2.23, m	2.24, m	2.24, m	2.27, m	2.28, m	2.27, m
7	5.80, br d (10.3)	5.80, br d (10.3)	5.79, dd (10.3, 1.3)	5.80, dd (10.4, 1.3)	5.82, br d (10.3)	5.82, br d (10.3)	5.82, br d (10.3)	5.80, dd (10.3, 1.2)	5.80, br d (10.1)	5.44, m
8	5.72, m	5.71, m	5.71, m	5.71, m	5.72, m	5.71, m	5.70, m	5.72, m	5.71, m	5.68, m
9	1.91, m	1.91, m	1.91, m	1.91, m	1.93[a], m	1.91, m	1.90, m	1.91, m	1.91, m	1.91, m
10a	1.70, m	1.69[a], m	1.69[a], m	1.69[a], m	1.69[a], m	1.69, m	1.67, m	1.70, m	1.68, m	1.64, m
10b	1.40, m	1.40, m	1.40, m	1.39, m	1.40, m	1.40, m	1.39, m	1.40, m	1.39, m	1.46, m
11a	1.82, m	1.80, m	1.82, m	1.81, m	1.89[a], m	1.87, m	1.87, m	1.82, m	1.81, m	1.87[a], m
11b	1.22, m	1.22, m	1.23, m	1.23, m	1.22, m	1.22, m	1.22, m	1.22, m	1.21, m	1.30, m
12a	2.00, m	1.67[a], m	1.06, d (7.5)	1.56[a], m	1.98[a], m	1.08, d (7.8)	1.53, m	2.08, m	2.00, m	2.01, m
12b		1.53, m					1.60, m			
13	3.89, m	1.06, t (7.5)		1.52[a], m	3.87, m		1.04, t (7.4)	3.78, m	3.96, m	3.87, m
14	1.73, s	1.74, s	1.69, s	1.73, s	1.64, s	1.60, s	1.64, s	1.73, s	2.17 m	1.62, s
16				0.90, t (7.3)						
17									1.02, t (7.3)	
NH	9.09, s	8.92, s	8.95, s	8.90, s	9.14, s	8.95, s	8.94, s	9.10, s	9.08, s	9.14, s
OH	5.51, d (8.0)	5.51, d (7.9)	5.49, d (8.0)	5.48, d (7.9)	5.43, d (8.5)	5.45, d (8.2)	5.40, d (8.3)	5.52, d (8.0)	5.54, d (7.9)	

[a] Due to spectral overlap in ^{1}H, assignment made using HSQC spectrum. [b] Atom numbering is adopted from salinosporamide A; additional carbons for **8** and **13** were assigned as C-16 and C-17, respectively.

Table 2. ^{13}C NMR Assignments for Compounds **3**, **4**, and **7**−**14** (DMSO-d_6)[a,b]

position	3	4	7	8	9	10	11	12	13	14
1	175.1, qC	175.7, qC	175.8, qC	175.9, qC	175.8, qC	177.2, qC	176.5, qC	175.0, qC	175.8, qC	174.9, qC
2	45.1, CH	49.1, CH	43.0, CH	47.4, CH	45.9, CH	44.0, CH	49.9, CH	46.3, CH	43.4, CH	44.5, CH
3	85.3, qC	86.1, qC	85.9, qC	86.1, qC	85.8, qC	86.3, qC	86.5, qC	85.2, qC	87.6, qC	85.5, qC
4	78.9, qC	78.6, qC	78.4, qC	78.6, CH	79.9, qC	79.8, qC	79.6, qC	78.9, qC	79.2, qC	74.7, qC
5	69.0, CH	69.1, CH	69.1, CH	69.1, CH	68.6, CH	68.6, CH	68.7, CH	69.0, CH	69.2, CH	32.5, CH_2
6	37.6, CH	37.6, CH	37.6, CH	37.7, CH	37.5, CH	37.5, CH	37.5, CH	37.6, CH	37.8, CH	29.8, CH
7	128.4, CH	128.4, CH	128.4, CH	128.5, CH	128.4, CH	128.5, CH	128.5, CH	128.3, CH	128.4, CH	131.1, CH
8	127.7, CH	127.6, CH	127.7, CH	127.7, CH	127.7, CH	127.6, CH	127.7, CH	127.7, CH	127.6, CH	127.6, CH
9	24.5, CH_2	24.5, CH_2	24.5, CH_2	24.5, CH_2	24.5, CH_2	24.5, CH_2	24.5, CH_2	24.5, CH_2	24.5, CH_2	24.4, CH_2
10	20.9, CH_2	20.9, CH_2	20.9, CH_2	21.0, CH_2	20.8, CH_2	20.8, CH_2	21.0, CH_2	20.9, CH_2	20.9, CH_2	20.2, CH_2
11	25.2, CH_2	25.3, CH_2	25.3, CH_2	25.3, CH_2	25.0, CH_2	25.2, CH_2	25.2, CH_2	25.2, CH_2	25.3, CH_2	28.6, CH_2
12	27.8, CH_2	17.9, CH_2	7.2, CH_3	26.8, CH_2	31.2, CH_2	12.5, CH_3	20.9, CH_2	28.1, CH_2	29.3, CH_2	28.0, CH_2
13	42.8, CH_2	12.3, CH_3		20.3, CH_2	42.6, CH_2		12.0, CH_3	32.2, CH_2	42.7, CH_2	
14	19.2, CH_3	20.1, CH_3	18.6, CH_3	20.0, CH_3	16.3, CH_3	16.1, CH_3	16.3, CH_3	19.3, CH_3	26.0, CH_2	18.5, CH_3
15	168.3, qC	168.8, qC	168.8, qC	168.9, qC	168.4, qC	168.8, qC	168.9, qC	168.3, qC	168.5, qC	169.7, qC
16				14.0, CH_3						
17									7.9, CH_3	

[a] Multiplicity observed by multiplicity edited HSQC [b] Atom numbering is adopted from salinosporamide A; additional carbons for **8** and **13** were assigned as C-16 and C-17, respectively.

relative stereochemistry assigned to **7**. The optical rotation of **7** ($[\alpha]^{22}_D$ −63.8 (*c* 4.71, CH_3CN)) was of similar magnitude and direction to those of **3** and **4** ($[\alpha]^{22}_D$ −66.5 (*c* 2.00, CH_3CN) and −69.6 (*c* 2.51, CH_3CN), respectively); this, together with the relative stereochemistry assignment, suggests the same absolute configuration for **3**, **4**, and **7**. Salinosporamide E (**8**; R = propyl) was detected in the crude extract by LC-MS (*m*/*z* 294.17) and isolated in small quantities. By comparison of spectroscopic data, the structure was confirmed to be identical to a semisynthetic derivative reported previously.[13] As the procedure for the semisynthesis of **8** from **3** would not be expected to introduce any changes in stereochemistry, it was concluded that the absolute configurations of salinosporamides A and E are identical.

A series of analogues with *S* configuration at C-2 was also characterized. The molecular formula of salinosporamide F (**9**) was established as $C_{15}H_{20}NO_4Cl$ by HRESI (*m*/*z* 314.1158 $[M + H]^+$, Δ_{calc} = −0.4 ppm), and the pseudomolecular ion displayed a characteristic isotope peak at *m*/*z* 316 with a ratio of 3:1 in intensity, consistent with the presence of one chlorine atom. Comparison of the ^{1}H NMR spectrum of **9** with that of **3** indicated that the compounds are nearly identical (Table 1), although several resonances differed slightly in chemical shift and ^{1}H−^{1}H coupling constants (specifically, H-5, OH-5, and H-14), suggesting that **9** was a diastereomer of **3**. This hypothesis was confirmed by X-ray crystallography, which unambiguously established **9** as the C-2 epimer of **3** (Figure 1). NOE data for **9** corresponded well with the configuration observed in the X-ray crystal structure. Specifically, a strong correlation between the H_2-12 methylene protons and the H_3-14 methyl protons, a weak correlation between the H-2 methine proton and the H_3-14 methyl protons, and a strong correlation from H_3-14 to H-5 are consistent with the placement of the C-14 methyl, the chloroethyl group, and C-5 on the same face of the bicyclic γ-lactam-β-lactone ring system. Comparison of the ^{13}C NMR spectra of **3** and **9** revealed that the chemical shift of C-12 is downfield-shifted by 3.4 ppm in the 2*S* isomer **9** compared to the 2*R* isomer **3** (Table 2). In addition, C-14 is upfield-shifted by 2.9 ppm in **9** compared with **3**. These spectroscopic trends were diagnostic in assigning the stereochemistry for the two other diasteromeric pairs, **7** and **10**, and **4** and **11**, as discussed below.

The HRESIMS measurement for salinosporamide G (**10**; *m*/*z* 266.1388 $[M + H]^+$, Δ_{calc} = −1.8 ppm) indicated a molecular formula of $C_{14}H_{19}NO_4$, consistent with a structural isomer of **7**.

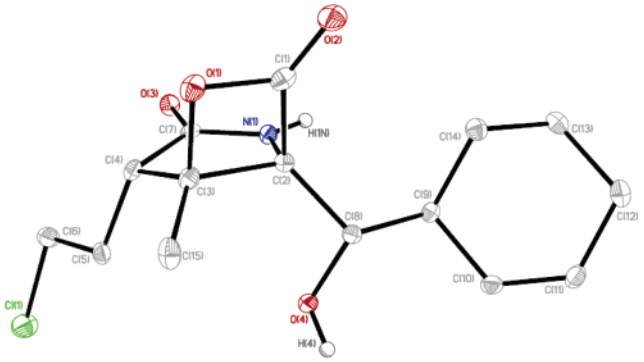

Figure 1. Computer-generated ORTEP plot of the x-ray crystal coordinates for **9**, with atom numbering according to the CIF file, which has been deposited with the Cambridge Crystallographic Data Center. Copies of the data can be obtained free of charge on application to the Director, CCDC, 12 Union Road, Cambridge, CB2 1EZ, UK (fax: +44-(0)1223-336033 or e-mail: deposit@ccdc.cam.ac.uk).

Similarities in their ^{1}H NMR spectra (Table 1) supported this hypothesis. The ^{1}H and ^{13}C chemical shift patterns established for the C-2 diastereomers **3** and **9** were also observed for **7** and **10**. These data, together with those obtained from NOESY spectra, were used to propose the stereochemical assignment of **10** as 2*S*. Specifically, a weak NOE correlation was detected from H_3-14 to H-2, whereas strong correlations were observed from H_3-14 to H_3-12 and H-5, indicating that the C-14 and C-2 methyl groups and C-5 are on the same face of the bicyclic γ-lactam-β-lactone ring system. Furthermore, the H-5/H-6 coupling constant was similar to that of **3** and other analogues. Together, these data indicated that **10** is the C-2 epimer of **7**.

For salinosporamide H (**11**), the molecular formula of $C_{15}H_{21}NO_4$ was established by HRESI (*m*/*z* 280.1556 $[M + H]^+$, Δ_{calc} = 2.7 ppm), indicating that **11** was a structural isomer of **4**. Correlations observed in 2D COSY spectra and ^{13}C chemical shifts of **11** were similar to those of **4**. Although no HMBC correlation was observed to the C-15 β-lactone carbonyl, the presence of the β-lactone ring may be inferred by both the molecular formula and the overall spectroscopic similarities to **4** for other ^{1}H and ^{13}C resonances in the bicyclic ring system. Due to the small amount of sample isolated, no NOE correlations were observed despite repeated attempts. However, the ^{1}H and ^{13}C NMR chemical shift trends observed for C-2 epimers **3** and **9** were also seen when NMR assignments for **4** and **11** were compared (Tables 1 and 2). Notably, ^{1}H NMR signals for H-5, OH-5, and H-14 of **11** were upfield-shifted, the ^{13}C NMR chemical shift of C-12 was downfield-shifted by 3.0 ppm, and the chemical shift of C-14 was upfield-shifted by 3.8 ppm compared to **4** (Table 2). As these chemical shift patterns were observed for all other compounds assigned with the *S* stereochemistry at C-2, the data indicated that **11** is the C-2 epimer of **4**.

Bromosalinosporamide (**12**) was extensively characterized using spectroscopic methods including HR-APCI mass spectrometry, ^{1}H NMR, ^{13}C NMR, and two-dimensional NMR methods. A molecular formula of $C_{15}H_{20}NO_4Br$ was calculated from the HR-APCIMS measurement (*m*/*z* 358.0647 $[M + H]^+$, Δ_{calc} = −1.9 ppm). The molecular ion contained an isotopic ratio of 1:1 for $[M + H]^+$ peaks at *m*/*z* 358 and 360, appropriate for a compound containing one bromine atom and no additional halogens. Both ^{1}H and ^{13}C NMR assignments for the compound compared well with assignments for **3** and literature values for brominated alkyl groups.[19] Notably, the chemical shift for C-13 of **12** was 10 ppm upfield compared to **3**, consistent with replacement of chlorine with bromine. The substitution of bromine for chlorine in the chloroethyl group of **3** is the expected metabolite when the organism is grown in media enriched in NaBr and with no addition of NaCl. With respect to stereochemistry, strong NOE correlations were observed between

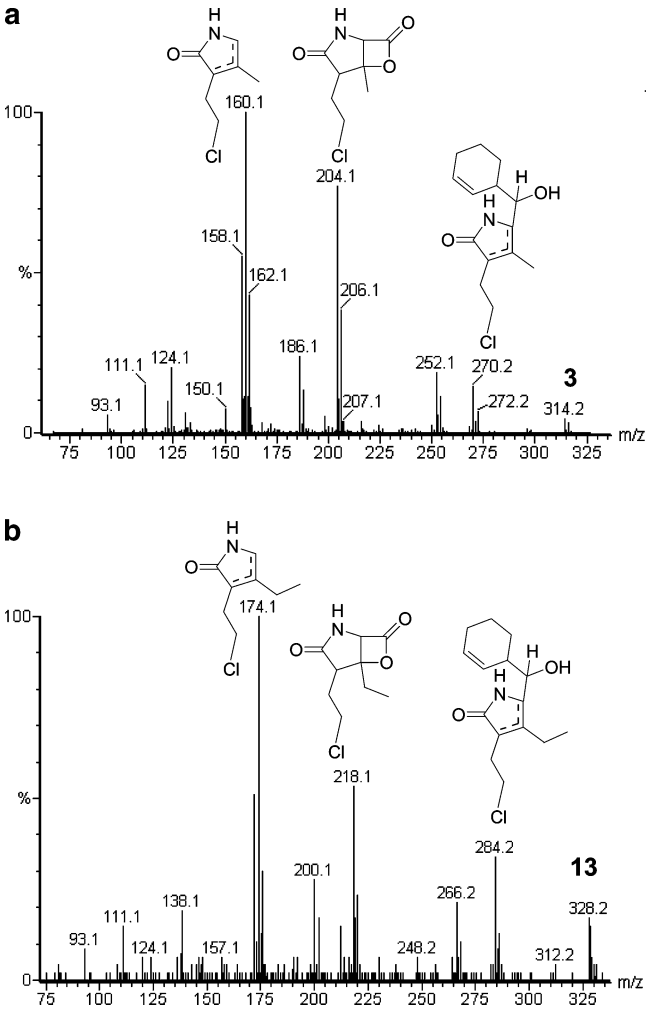

Figure 2. MS−MS fragmentation pattern observed for **3** (a) and **13** (b).

H_3-14 and H-5 as well as from H_3-14 to H-2, and the H-5/H-6 coupling constant compared favorably to those of **3** and **9**, for which the configurations were established by X-ray. These data support the relative stereochemistry assigned to **12**. We have previously established that the biological activity of **12** is almost identical to that of **3** in five in vitro assays and that changes in stereochemistry have a significant impact on the SAR of the salinosporamides.[13] The collective data suggest that the absolute stereochemistry of **12** is the same as **3**.

The structural characterization of salinosporamide I (**13**) is supported by HRESIMS measurements (*m*/*z* 328.1309 $[M + H]^+$), suggesting a molecular formula of $C_{16}H_{22}ClNO_4$, consistent with the addition of one methylene group to **3**. The position of the additional methylene group was initially suggested by comparison of the fragmentation patterns observed by MS−MS experiments on **3** and **13** (Figure 2). The two most intense ions of **3** (*m*/*z* 204.1, 160.1) were assigned to fragments generated by loss of the cyclohexenyl carbinol substituent, followed by decarboxylation, respectively. Incorporation of 14 additional mass units into these two ions in the MS−MS spectrum of **13** suggested that the additional methylene group was localized within either the C-2 or C-3 substituent. By comparison of the ^{1}H NMR spectra of **13** and **3**, it was clear that **13** bears an ethyl group in place of the methyl group at the bridgehead position C-3. Specifically, the methyl singlet at 1.73 ppm in the ^{1}H NMR spectrum of **3** was absent from the ^{1}H NMR spectrum of **13**, which instead contained a triplet methyl group at 1.02 ppm (H_3-17) and a 2H multiplet at 2.17 ppm (H_2-14), both consistent with an ethyl group. Prior to this discovery, only hydrogen (**2** and its analogues) or a methyl group (**3** and **5**

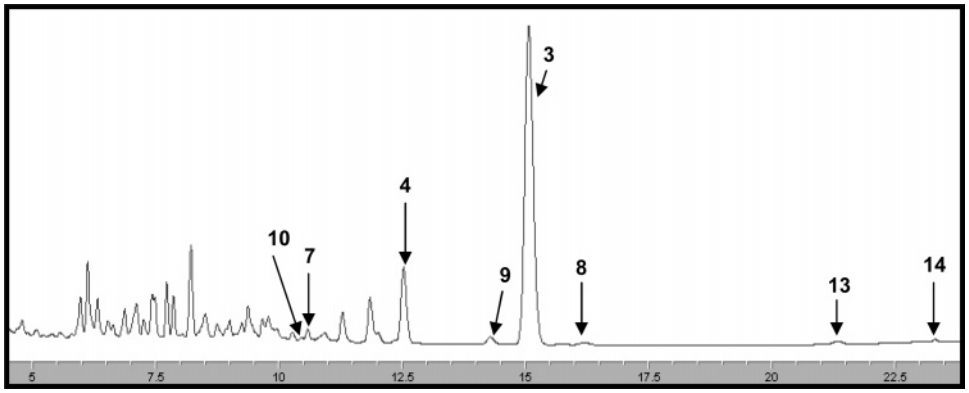

Figure 3. Representative analytical HPLC chromatogram (210 nm) of the crude extract produced from strain NPS000465.

and their analogues) had been reported at this position for compounds within the γ-lactam-β-lactone family. NOE correlations from H_2-14 to H-5 and H-2, along with an H-5/H-6 coupling constant that compared favorably with compound **3**, indicated that the relative stereochemistry of **13** is the same as compound **3**.

The assignment of salinosporamide J (**14**) as the C-5 deshydroxyl analogue of **3** is supported by a molecular formula of $C_{15}H_{20}NO_3$-Cl, as determined by HRESIMS (*m/z* 298.1214 $[M + H]^+$, $\Delta_{calc} =$ 1.5 ppm). The doublet in the 5.5 ppm range of the ^{1}H NMR spectrum was absent and a new methylene group was detected via the multiplicity-edited HSQC (δ_H 1.82, m; δ_C 32.5, CH_2). The new methylene protons showed COSY correlations to H-6 and HMBC correlations to C-7 and the C-15 β-lactone carbonyl, collectively establishing the methylene group at C-5. The NOE correlation from H_3-14 to H-2 was notably stronger than the correlation from H_3-14 to H-12. A strong correlation was also observed from H_3-14 to H_2-5. These data supported the relative stereochemical assignment about the bicylcic ring system. The stereochemistry at C-6 of the cyclohexene ring was not determined. This molecule represents the second in a family of γ-lactam-β-lactone natural products with a methylene group at this position, the first having been reported as an analogue of **5**.[12]

In order to approximate the percentage of the various salinosporamide congeners that were present in the crude extract, a representative sample produced using standard fermentation conditions was analyzed by LC-MS (Figure 3). The major component of the crude extract was parent compound **3**, for which the peak integrated to 38.5% of the sample (UV area % at 210 nm). The crude extract also contained **4** (6%) as a major analogue, along with diastereomer **9** (~1%), methyl analogue **7** (~1%), and propyl analogue **8** (0.3%). The presence of **10**, **13**, and **14** was detected in the total ion chromatogram, and these compounds were estimated to comprise <0.5%; however, the percentages were not more accurately determined due to coelution with other compounds in the crude extract. Analogues **11** and **12** were not detected in the extract produced under our standard fermentation conditions and have only been isolated from extracts produced by fermentation in the presence of NaBr. The isolated yield of **11** was only 0.03% from dried extract weight; in contrast, the isolated yields for compounds **12** and **4** were 2.5% and 3.2%, respectively, calculated from dried crude extract weight. Of the eight new salinosporamides described herein, six represent modifications at the C-2 substituent, three of which are C-2 epimers (**9**, **10**, and **11**). HPLC data from fermentation culture extracts sampled over time (data not shown) indicated that the ratio of **9** to **3** was fairly constant throughout the fermentation cycle, suggesting that C-2 epimers are not post-biosynthetically racemized.

Semisynthesis of Thioester Derivatives. Despite our thorough examination of *S. tropica* extracts, no thioester analogues of the salinosporamides were identified. This is in direct contrast with omuralide (**1**), which is found in nature as its thioester precursor lactacystin (**2**),[7,8] and with more recent reports of related compounds (e.g., **5** and **6**).[12] Thus, in addition to the eight new salinosporamides obtained through fermentation, a series of thioester analogues was generated by derivatization of **3** and **4**. Salinosporamide A (**3**) was treated with methyl-3-mercaptopropionate to produce **15**, which was slowly and partially converted to **16**. This is consistent with previous observations that β-lactone ring opening may be followed by nucleophilic displacement of chlorine to produce a cyclic ether.[13] The mixture was separated by HPLC, which allowed the compounds to be independently screened for biological activity. Salinosporamide B (**4**) was cleanly converted to **17**. Conversion of **3** to *N*-acetyl-L-cysteine methyl ester (glutathione) adduct **18** was also followed by chlorine elimination to produce **19**, and as in the case of **15** and **16**, it was possible to isolate both **18** and **19** as pure compounds.

Table 3. IC_{50} Values for Cytotoxicity against RPMI 8226 Cells and Inhibition of the CT-L Activity of Purified Rabbit 20S Proteasome

compound	CT-L activity IC_{50} (nM)	RPMI 8226 IC_{50} (nM)
3[13]	2.6 ± 0.2	8.2 ± 2.0
4[13]	26 ± 6.7	6100 ± 3300
1[13]	57 ± 5.8	3300 ± 1600
14	52 ± 2	250 ± 20
15	9.3 ± 1.5	11 ± 2
16	230 ± 35	7500 ± 1100
17	50 ± 10	8000 ± 3400
18	4.0 ± 0	9.7 ± 1.5

Cytotoxicity against RPMI 8226 Cells and Inhibition of Chymotrypsin-like (CT-L) Activity of Rabbit 20S Proteasomes. The inhibitory effects of omuralide (**1**), salinosporamide A (**3**), **4**, and **7**−**13** on purified rabbit 20S proteasomes have been reported previously.[9,13] In that study, we showed that the two most potent compounds with respect to inhibition of CT-L activity were halogenated compounds **3** and **12**. We have recently proposed a mechanistic role for the halogen atom as a leaving group, with implications for irreversible inhibition of the proteasome.[13,14] Removal of the halogen, C-2 epimerization, and extension of the carbon chain of the substituent at the C-3 ring junction resulted in less potent analogues.[13] IC_{50} values for cytotoxicity against RPMI 8226 cells and inhibition of the CT-L activity of purified rabbit 20S proteasome for compounds **14**−**18** are summarized in Table 3 along with data for **1**, **3**, and **4** for comparative analysis. In terms of inhibition of CT-L activity, analogue **14** (C-5H_2) was 20-fold less potent than **3** but significantly more active than the keto-C-5 and epi-C-5-OH analogues of **3** reported previously ($IC_{50} = 8$ and >20 μM, respectively).[13] Thus, reduction of the C-5 hydroxyl group to a methylene group was better tolerated than epimerization or oxidation. The X-ray crystal structure of **3** in complex with the yeast 20S proteasome indicates that the C-5-OH group of **3** is involved in hydrogen-bonding interactions with the enzyme, while the C-5-OH epimer and keto compounds are expected to introduce

steric interactions that are not well tolerated.[14] For **14**, this hydrogen-bonding potential is lost, but problematic steric interactions would not be expected, in agreement with the trends in the assay data (IC_{50} **3** < **14** (C-5H_2) ≪ keto-C-5 < epi-C-5-OH).

Thioester derivatives **15** and **18** were potent 20S proteasome inhibitors, with IC_{50} values only 3.6- and 1.5-fold higher than that of **3**, respectively. Similarly, thioester **17** was only 2-fold less active than its parent, **4**. The results of studies on omuralide (**1**) and lactacystin (**2**) by Dick et al. indicate that β-lactone **1** is born from thioester **2** *in situ* and represents the species that enters the cell and reacts with the proteasome.[15,16] The collective data presented below suggest that the thioesters may directly inhibit the proteasome, albeit with reduced potency. Thus, the slightly weaker potencies of thioester analogues of **3** and **4** may result from the presence of a mixture of species produced *in situ*, including (i) the thioester itself; (ii) the corresponding β-lactone; and in the case of **3**, (iii) the cyclic ether (i.e., **16** and **19**, derived from **15** and **18**, respectively). These cyclic ethers, which result from chlorine elimination, *cannot be converted back to* β*-lactone* ***3***. Interestingly, while **16** was 100-fold less active than **3**, it retained submicromolar potency as a proteasome inhibitor. As it is not possible to generate a β-lactone ring from **16**, these data indicate that the thioester species reacts directly with the proteasome. We further observed that the thioester analogues were cytotoxic against RPMI 8226 cells *in vitro*. Significantly, thioester **16** has similar potency (i.e., IC_{50} in the micromolar range) to **1** and **4** in this assay. Assuming that cell permeation is required for this class of compounds to induce cytotoxicity (putatively via proteasome inhibition), our results suggest that thioester analogues can directly enter the cell. This result is in apparent contrast to the findings of Dick et al., wherein the thioester lactacystin is reported to convert to the β-lactone prior to cell entry.[15,16] Nevertheless, the significantly enhanced potencies of **15** and **18** as compared to **16** confirm the importance of the potential for β-lactone ring formation and the presence of an intact chloroethyl group. Recent X-ray crystallographic analysis of **3** in complex with the yeast proteasome indicates that the β-lactone reacts with the N-terminal threonine residue of the proteasome, followed by intramolecular nucleophilic displacement of chlorine, which plays a key role in the mechanism of irreversible inhibition.[14] While thioesters may give rise to β-lactone rings (which acylate the proteasome), the thioester form of **3** may undergo the competing reaction of chlorine elimination, thereby disabling the molecule's full inhibitory potential. It is no wonder that thioester analogues of the salinosporamides have not been found in nature.

Experimental Section

General Experimental Procedures. Optical rotations were measured on a Rudolph Autopol III polarimeter using a 4 × 100 mm sample cell. UV spectra were obtained with a Beckman Coulter DU 640 spectrophotometer or from analytical HPLC analysis of the purified compound using an Agilent HP1100 HPLC equipped with an Agilent PDA detector; the mobile phase was a mixture of acetonitrile (CH_3-CN) and H_2O. IR spectra were acquired using a Nicolet Magna-IR 550 Series II spectrometer (NaCl disk). NMR spectra were collected using a 500 MHz Bruker Avance NMR spectrometer with an inverse probe equipped with *x*,*y*,*z*-gradients, except for the ^{13}C NMR spectrum, which was acquired with a broad-band observe probe. All NMR data were acquired at 300 K in DMSO-d_6, referenced to 2.49 ppm in the proton spectra and 39.50 ppm in carbon spectra. High-resolution mass spectra and MS−MS data were acquired using a Micromass Q-Tof2 mass spectrometer with ES+ or APCI+ ionization. HRESI spectra were referenced using a polyethylene glycol polymer mixture, which was co-injected during acquisition as an internal accurate mass standard. MS−MS fragmentation experiments were performed using ES+ ionization followed by fragmentation using 20 eV collision energy with Ar as the collision gas. Additional ESIMS and crude extract analysis (Figure 3) experiments were collected using an Agilent HP1100 HPLC equipped with an Agilent PDA detector and an 1100 series MSD Agilent mass spectrometer. Normal-phase flash chromatography was performed using either a Biotage Flash 40i system with Flash 40M cartridge (KP-Sil Si, 32−63 μm, 90 grams) or open flash columns (250 cm^3 Si gel, column dimensions 2.5 cm diameter by 15 cm length). HPLC was performed on a Gilson HPLC equipped with a Gilson 215 fraction collector and Agilent PDA detector. For normal-phase separations, an evaporative light scattering detector (ELSD; Sedere) was used to monitor the purification process. Unless otherwise specified, a Phenomenex Luna Si (10 μm, 100 Å; 250 × 21.2 mm i.d.) column was used for normal-phase HPLC at a flow rate of 25 mL/min. For RP HPLC separations, an Eclipse XDB-C18, 5 μm, 150 × 21 mm i.d. column was used at a flow rate of 14.5 mL/min. HPLC solvents were obtained from Fisher Scientific and VWR, and water used for HPLC was filtered through a NANOpure Infinity ultrafilter. Deuterated solvents were obtained from Cambridge Isotope Laboratories, Inc. (Andover, MA).

Purified rabbit muscle 20S proteasome (1 mg/mL) in 50 mM HEPES, pH 7.6, 150 mM NaCl, and 1 mM DTT was purchased from Boston Biochem (Cambridge, MA). Fluorogenic peptide substrate Suc-LLVY-AMC (Boston Biochem, Cambridge, MA) was used to monitor the CT-L activity of the 20S proteasome *in vitro*. The peptide substrate was prepared in 100% DMSO as 10 mM stock solution and stored at −20 °C. The human multiple myeloma cell line RPMI 8226 (CCL-155) was purchased from ATCC (Manassas, VA). The cells were maintained in RPMI 1640 medium supplemented with 10% heat inactivated FBS, 100 units/mL penicillin, 100 μg/mL streptomycin, 2 mM L-glutamine, and 1 mM sodium pyruvate at 37 °C, 5% CO_2, and 95% humidified air. Omuralide was obtained from CalBiochem (San Diego, CA). All other chemical reagents were obtained from Sigma-Aldrich, except for DMSO, which was obtained from EM Sciences Corp. and Fisher Scientific.

Microorganism. The producing culture, *Salinispora tropica* NPS000465, was isolated from a sediment sample collected from Cross Harbor, Abaco, Bahamas, by Jensen, Dwight, and Fenical (1991).[20] Strain NPS000465 was deposited with the American Type Culture Collection and assigned the accession number PTA-5275.

Media and Culturing Conditions for 3, 4, 7−10, 13, and 14. Aliquots (4 mL) of seed cultures of *S. tropica* NPS000465 were transferred to four hundred 500 mL flasks containing 100 mL of production medium consisting of the following per liter of deionized water: starch, 10 g; yeast extract, 4 g; Hy-Soy, 4 g; ferric sulfate, 40 mg; potassium bromide, 100 mg; calcium carbonate, 1 g; and synthetic sea salt, 30 g. The production cultures were incubated at 28 °C and 250 rpm for 1 day. Approximately 2 g of sterile Amberlite XAD-7 resin was added to the production cultures. The production cultures were further incubated for 5 days. The resin was recovered from the broth and extracted with ethyl acetate. The extract was dried *in vacuo*. The dried extract (8 g) was then processed for the recovery of **7**−**10**, **13**, and **14**.

Media and Culturing Conditions for 3, 4, 11, and 12. For enrichment of the production of **12** in the fermentation, the synthetic sea salt in the production media was replaced with sodium bromide. Aliquots (4 mL) of the seed cultures of *S. tropica* NPS000465 were transferred to one hundred and fifty 500 mL flasks containing 100 mL of production medium containing sodium bromide (30 g/L) instead of synthetic sea salt. Approximately 2 g of sterile Amberlite XAD-7 resin was added to the production cultures. The production cultures were incubated at 28 °C and 250 rpm for 6 days. The resin was recovered from the broth and extracted with ethyl acetate. The extract was dried *in vacuo*. The dried extract (2.4 g) was then processed for the recovery of **11** and **12**.

Purification of 7−10, 13, and 14. The crude extract containing **3**, **4**, **7**−**10**, **13**, and **14** was processed by flash chromatography using a Biotage Flash system. The flash chromatography was developed by the following step gradient: (i) hexanes (1 L); (ii) 10% EtOAc in hexanes (1 L); (iii) 20% EtOAc in hexanes, first elution (1 L); iv) 20% EtOAc in hexanes, second elution (1 L); (v) 20% EtOAc in hexanes, third elution (1 L); (vi) 25% EtOAc in hexanes (1 L); (vii) 50% EtOAc in hexanes (1 L); (viii) EtOAc (1 L). Generally, fractions from step gradient v, vi, and vii were enriched in **3** but also contained minor analogues **4**, **7**−**10**, **13**, and **14** in varying amounts. Fractions containing compounds **7**−**10**, **13**, and **14** were further purified by normal-phase HPLC using an isocratic solvent system of 24% EtOAc/hexanes followed by a 100% EtOAc. Compound **14** eluted first after 7.5 min, followed by **13** and **9**, which coeluted as a single peak at 11 min.

Compound **3** eluted as a major, broad peak (14 min) followed by compound **8**, which eluted 22 min into the isocratic portion of the run. Finally, compound **4** eluted at 31 min, during the 100% EtOAc elution, followed by coelution of compounds **7** and **10** at 32 min.

A sample containing a 9:1 mixture of **9** and **13** was further separated using RP HPLC in which the solvent gradient increased linearly from 15% CH_3CN/85% H_2O to 100% CH_3CN over 23 min. Compound **9** eluted at 17.5 min, while compound **13** eluted at 19 min under these conditions.

Fractions enriched in **8** were further processed by normal-phase HPLC using a 27 min linear gradient from 15% hexanes/85% EtOAc to 100% EtOAc. Compound **8** eluted after 15 min. The same method was also used for fractions enriched in **14**, which eluted at 7.5 min.

A reversed-phase isocratic solvent system of 27% CH_3CN/63% H_2O was used to separate compounds **10** and **7**, which eluted after 14 and 16 min, respectively.

To minimize hydrolysis of the β-lactone ring, which may occur during exposure to the aqueous mobile phase, fractions from RP HPLC containing compounds of interest were evaporated under reduced pressure without heating on a rotary evaporator immediately after being fractionated. If hydrolysis product still formed under these conditions, the resulting sample was further purified on a normal-phase Si plug (1 cm diameter by 2 cm height) using a solvent mixture of 30% acetone/70% hexanes or 20% EtOAc/80% hexanes.

Salinosporamide D (7): white solid; $[\alpha]^{22}_D$ −63.8 (*c* 4.71, CH_3CN); UV (CH_3CN) λ_{max} (log ϵ) 223 (sh) (3.06), 208 (3.06) nm; IR (NaCl) ν_{max} 3383, 2936, 1825, 1713 cm^{-1}; ^1H NMR (DMSO-d_6), see Table 1; ^{13}C NMR (DMSO-d_6), see Table 2; HRESIMS *m/z* 266.1396 $[M + H]^+$ (calcd for $C_{14}H_{20}NO_4$, 266.1392).

Salinosporamide E (8): white solid; $[\alpha]^{22}_D$ −60.0 (*c* 0.1, CH_3CN); ^1H NMR (DMSO-d_6), see Table 1; ^{13}C NMR (DMSO-d_6), see Table 2; HRESIMS, *m/z* 294.1713 $[M + H]^+$ (calcd for $C_{16}H_{24}NO_4$, 294.1705).

Salinosporamide F (9): white solid; $[\alpha]^{22}_D$ −108.9 (*c* 8.78, CH_3CN); UV (CH_3CN) λ_{max} (log ϵ) 223 (sh) (3.05), 206 (3.16) nm; IR (NaCl) ν_{max} 3452, 2926, 1808, 1701 cm^{-1}; ^1H NMR (DMSO-d_6), see Table 1; ^{13}C NMR (DMSO-d_6), see Table 2; HRESIMS *m/z* 314.1158 $[M + H]^+$ (calcd for $C_{15}H_{21}NO_4Cl$, 314.1159).

Salinosporamide G (10): white solid; $[\alpha]^{22}_D$ −54.5 (*c* 1.10, CH_3CN); UV (CH_3CN) λ_{max} (log ϵ) 218 (sh) (3.08), 209 (3.09) nm; IR (NaCl) ν_{max} 3360, 2931, 1820, 1701 cm^{-1}; ^1H NMR (DMSO-d_6), see Table 1; ^{13}C NMR (DMSO-d_6), see Table 2; HRESIMS *m/z* 266.1388 $[M + H]^+$ (calcd for $C_{14}H_{20}NO_4$, 266.1392).

Salinosporamide I (13): white solid; $[\alpha]^{22}_D$ −20.0 (*c* 0.90, CH_3CN); UV (CH_3CN) λ_{max} (log ϵ) 220 (sh) (2.99), 205 (3.19) nm; ^1H NMR (DMSO-d_6), see Table 1; ^{13}C NMR (DMSO-d_6), see Table 2; HRESIMS *m/z* 328.1309 $[M + H]^+$ (calcd for $C_{16}H_{23}NO_4Cl$, 328.1316).

Salinosporamide J (14): white solid; $[\alpha]^{22}_D$ −120.0 (*c* 0.30, CH_3CN); UV (CH_3CN) λ_{max} (log ϵ) 230 (sh) (3.19), 217 (3.21) nm; ^1H NMR (DMSO-d_6), see Table 1; ^{13}C NMR (DMSO-d_6), see Table 2; HRESIMS *m/z* 298.1214 $[M + H]^+$ (calcd for $C_{15}H_{21}NO_3Cl$, 297.1131).

Purification of 11 and 12. The crude extract containing **3**, **4**, **11**, and **12** was dissolved in acetone, loaded on a Si flash column, and washed with a step gradient of hexanes/EtOAc, increasing in the percentage of EtOAc in steps of 5% (100 mL of solvent per step). The majority of **11** and **12** eluted in 60% hexanes/40% EtOAc, and this mixture was further separated by RP HPLC chromatography using an isocratic solvent system consisting of 35% CH_3CN/65% H_2O. Under these conditions, **11** eluted at 11.0 min, followed by **4**, which eluted at 12.0 min. Traces of **3** eluted at 23.5 min, and **12** eluted last, 25.5 min into the run. Sample containing compound **12** also included hydrolysis product and was washed through a Si plug using a solvent mixture of 20% EtOAc/80% hexanes, resulting in pure **12**.

The fractions containing compound **11** described above were further purified by normal-phase HPLC (Phenomenex Luna Si, 10, 100 Å 250 × 10 mm i.d.) using a solvent gradient increasing from 100% hexanes to 100% EtOAc over 20 min at a flow rate of 4 mL/min. Compound **11** eluted as a pure compound after 11.5 min.

Salinosporamide H (11): white solid; UV (CH_3CN/H_2O) λ_{max} (log ϵ) 221 (sh) nm; ^1H NMR (DMSO-d_6), see Table 1; ^{13}C NMR (DMSO-d_6), see Table 2; HRESIMS *m/z* 280.1556 $[M + H]^+$ (calcd for $C_{15}H_{22}NO_4$, 280.1549).

Bromosalinosporamide (12): white solid; $[\alpha]^{22}_D$ −51.6 (*c* 0.95, CH_3CN); UV (CH_3CN) λ_{max} (log ϵ) 220 (sh) (3.05), 205 (3.25) nm; IR (NaCl) ν_{max} 3365, 2918, 1811, 1702 cm^{-1}; ^1H NMR (DMSO-d_6), see Table 1; ^{13}C NMR (DMSO-d_6), see Table 2; HRAPCIMS *m/z* 358.0647 $[M + H]^+$ (calcd for $C_{15}H_{21}NO_4Br$, 358.0654).

Crystallization and X-ray Crystallographic Analysis of 9. Crystalline **9** was obtained using a vapor diffusion method. Compound **9** (15 mg) was dissolved in 100 μL of acetone in a 1.5 mL V-bottom HPLC vial. This vial was then placed inside a larger sealed vessel containing 1 mL of pentane. Crystals suitable for X-ray crystallography experiments were observed along the sides and bottom of the inner vial after 48 h of incubation at 4 °C. Crystallography data were collected on a Bruker SMART APEX CCD X-ray diffractometer ($F(000) = 2656$, Mo Kα radiation, $\lambda = 0.71073$ Å, $\mu = 0.264$ mm^{-1}, $T = 100$ K) at the University of California, San Diego Crystallography Lab. The refinement method used was full-matrix least-squares on F^2 (SHELXTL, Sheldrick, 1997). Crystal data for salinosporamide F (**9**): $C_{15}H_{20}ClNO_4$, MW = 313.77, tetragonal, space group *P*4(1)2(1)2, $a = 11.4901(3)$ Å, $c = 46.444(2)$ Å, vol = 6131.6(3) $Å^3$, $Z = 16$ (two identical molecules in the asymmetric unit), Flack parameter -0.04 ± 0.05, $\rho_{calcd} = 1.360$ g cm^{-3}, crystal size 0.30 × 0.15 × 0.07 mm^3, θ range 1.75−26.00°, 35 367 reflections collected, 6025 independent reflections ($R_{int} = 0.0480$), *R* indices: $R_{1(all)} = 0.0449$, $wR_{2(all)} = 0.0827$, GOF = 1.060.

Synthesis of 15 and 16 from 3. Salinosporamide A (**3**, 30 mg, 0.096 mmol) was dissolved in CH_2Cl_2 (9 mL) in a scintillation vial (20 mL) to which triethylamine (40 μL, 0.29 mmol), methyl-3-mercapto propionate (57.6 mg, 0.48 mmol), and a magnetic stir bar were added. The reaction mixture was stirred at room temperature for about 4 h. The solvent was evaporated from the reaction mixture to yield a mixture of **15** and **16** (19:1), which was separated by RP HPLC with a solvent gradient of 35% to 90% H_2O/CH_3CN over 17 min, 90 to 100% CH_3CN over 1 min, holding at 100% CH_3CN for 1 min, at a flow rate of 14.5 mL/min. A diode array detector was used to monitor the purification process, with a primary wavelength of 210 nm.

Compound 15: colorless gum; $[\alpha]^{22}_D$ −26.0 (*c* 0.005, $CHCl_3$); UV (CH_3CN/H_2O) λ_{max} 240 (sh) nm; IR (NaCl) ν_{max} 3340, 2944, 1740 cm^{-1}; ^1H NMR (DMSO-d_6) δ 8.41 (1H, s, NH), 5.77 (1H, brd, $J = 10.5$ Hz, H-7), 5.62 (1H, m, H-8), 5.14 (1H, d, $J = 7.0$ Hz, OH), 4.97 (1H, s, OH), 3.82 (2H, m, H_2-13), 3.76 (1H, brt, H-5), 3.59 (3H, s, CO_2Me), 2.95 (2H, m, H_2-1′), 2.71 (1H, brt, H-2), 2.56 (2H, m, H_2-2′), 2.12 (1H, brs, H-6), 1.92 (1H, m, H-11a), 1.85 (2H, brs, H_2-9), 1.75 (1H, m, H-10a), 1.61 (1H, m, H-10b), 1.42 (3H, s, H_3-14), 1.31 (1H, m, H-11b); ^{13}C NMR (DMSO-d_6) δ 201.1 (C, C-15), 178.3 (C, C-1), 171.8 (C, C-3′), 129.2 (CH, C-7), 127.2 (CH, C-8), 80.4 (C, C-3), 80.1 (C, C-4), 75.4 (C, C-5), 51.5 (CH_3, C-4′), 48.0 (CH, C-2), 44.4 (CH_2, C-13), 38.1 (CH, C-6), 33.1 (CH_2, C-2′), 27.7 (CH_2, C-12), 27.0 (CH_2, C-11), 24.5 (CH_2, C-9), 23.3 (CH_2, C-1′), 21.4 (CH_2, C-10), 20.6 (CH_3, C-14); ESIMS *m/z* 434.0 $[M + H]^+$ and 456.0 $[M + Na]^+$; HRESIMS *m/z* 434.1413 $[M + H]^+$ (calcd for $C_{19}H_{29}ClNO_6S$, 434.1404).

Compound 16: colorless gum; UV (CH_3CN/H_2O) λ_{max} 220 (sh) nm; ^1H NMR (DMSO-d_6) δ 8.5 (1H, s, NH), 5.77 (1H, m, H-7), 5.65 (1H, m, H-8), 5.21 (1H, d, $J = 7.0$ Hz, OH), 3.73 (2H, t, $J = 8.0$ Hz, H_2-13), 3.68 (1H, t, $J = 8.0$ Hz, H-5), 3.59 (3H, s, CO_2Me), 2.96 (2H, t, $J = 7.0$ Hz, H_2-1′), 2.64 (1H, m, H-2), 2.56 (2H, m, H_2-2′), 2.17 (1H, m, H-6), 2.0 (2H, m, H_2-12), 1.85 (2H, m, H_2-9), 1.64 (1H, m, H-11a), 1.59 (1H, m, H-10a), 1.36 (3H, s, H_3-14), 1.31 (1H, m, H-10b), 1.23 (1H, m, H-11b); ESMS *m/z* 398.0 $(M + H)^+$ and 420.0 $[M + Na]^+$; HRESIMS *m/z* 398.1642 $[M + H]^+$ (calcd for $C_{19}H_{28}NO_6S$, 398.1637).

Synthesis of 17 from 4. Salinosporamide B (**4**, 25 mg, 0.0896 mmol) was dissolved in CH_2Cl_2 (9 mL) in a scintillation vial (20 mL) to which triethylamine (38 μL, 0.27 mmol), methyl-3-mercapto propionate (53.8, 0.45 mmol), and a magnetic stir bar were added. The reaction mixture was stirred at room temperature for about 4 h. The solvent was evaporated from the reaction mixture to yield **17**, which was further purified by normal-phase HPLC with a solvent gradient of 10% to 90% EtOAc/hexanes over 23 min, 90 to 100% EtOAc over 1 min, holding at 100% EtOAc for 3 min, at a flow rate of 14.5 mL/min.

Compound 17: colorless gum; $[\alpha]^{22}_D$ −12.8 (*c* 0.005, $CHCl_3$); UV (CH_3CN/H_2O) λ_{max} 240 (sh) nm; IR (NaCl) ν_{max} 3317, 2928, 1680 cm^{-1}; ^1H NMR (DMSO-d_6) δ 8.20 (1H, s, NH), 5.77 (1H, m, H-7), 5.63 (1H, m, H-8), 5.03 (1H, d, $J = 7.5$ Hz, OH), 4.78 (1H, s, OH), 3.76 (1H, t, $J = 7.0$ Hz, H-5), 3.59 (3H, s, CO_2Me), 2.94 (2H, t, $J = 7.0$ Hz, H_2-1′), 2.55 (2H, t, $J = 7.0$ Hz, H_2-2′), 2.34 (1H, t, $J = 7.0$ Hz, H-2), 2.1 (1H, m, H-6), 1.85 (2H, m, H_2-9), 1.61 (2H, m, H_2-12), 1.47 (2H, m, H-10a, 11a), 1.44 (3H, s, H_3-14), 1.40 (2H, m, H-10b, 11b), 0.97 (3H, t, $J = 7.5$ Hz, H_3-13); ^{13}C NMR (DMSO-d_6) δ 200.3 (C, C-15), 178.8 (C, C-1), 171.8 (C, C-3′), 129.3 (CH, C-7), 127.1 (CH, C-8), 80.7 (C, C-3), 79.9 (C, C-4), 75.5 (CH, C-5), 52.5 (CH, C-2),

51.5 (CH_3, C-4′), 38.1 (CH, C-6), 33.1 (CH_2, C-2′), 27.1 (CH_2, C-11), 24.5 (CH_2, C-9), 23.3 (CH_2, C-1′), 21.3 (CH_2, C-10), 21.2 (CH_3, C-14), 16.7 (CH_2, C-12), 13.5 (CH_3, C-13); ESMS *m/z* 400.1 $[M + H]^+$ and 422.1 $[M + Na]^+$; HRESIMS *m/z* 400.1798 $[M + H]^+$ (calcd for $C_{19}H_{30}NO_6S$, 400.1794).

Synthesis of 18 and 19 from 3. Salinosporamide A (**3**, 10 mg, 0.032 mmol) was dissolved in CH_2Cl_2 (9 mL) in a scintillation vial (20 mL) to which triethylamine (26.5 μL, 0.192 mmol), *N*-acetyl-L-cysteine methyl ester (17 mg, 0.096 mmol), and a magnetic stir bar were added. The reaction mixture was stirred at room temperature for about 4 h. The solvent was evaporated from the reaction mixture to yield a mixture of compounds **18** and **19** (19:1), which was further separated by normal-phase HPLC using the method described above for compound **17**.

Compound 18: colorless, viscous liquid; $[\alpha]^{22}_D$ +30.8 (*c* 0.005, $CHCl_3$); UV (CH_3CN/H_2O) λ_{max} 230 (sh) nm; IR (NaCl) ν_{max} 3379, 3239, 2928, 1693 cm^{-1}; ^1H NMR (DMSO-d_6) δ 8.45 (1H, brs, NH), 8.26 (1H, d, $J = 8.0$ Hz, NH), 5.77 (1H, m, H-7), 5.62 (1H, m, H-8), 5.15 (1H, d, $J = 7.0$ Hz, OH), 4.98 (1H, s, OH), 4.35 (1H, m, H-2′), 3.84 (2H, m, H_2-13), 3.77 (1H, t, $J = 7.0$ Hz, H-5), 3.63 (3H, s, CO_2-Me), 2.97 (2H, m, H_2-1′), 2.73 (1H, m, H-2), 2.11 (1H, m, H-6), 1.93 (2H, m, H_2-12), 1.84 (2H, m, H_2-9), 1.82 (3H, s, H_3-6′), 1.78 (1H, m, H-11a), 1.60 (2H, m, H_2-10), 1.43 (3H, s, H_3-14), 1.31 (1H, m, H-11b); ^{13}C NMR (DMSO-d_6) δ 200.6 (C, C-15), 178.4 (C, C-1), 170.9 (C, C-3′), 169.3 (C, C-5′), 129.1 (C, C-7), 127.2 (C, C-8), 80.4 (C, C-3), 80.2 (C, C-4), 75.4 (C, C-5), 52.1 (CH_3, C-4′), 51.5 (CH, C-2′), 47.9 (CH, C-2), 44.3 (CH_2, C-13), 38.1 (CH, C-6), 29.4 (CH_2, C-1′), 27.6 (CH_2, C-12), 27.0 (CH_2, C-11), 24.4 (CH_2, C-9), 22.2 (CH_3, C-14), 21.4 (CH_2, C-10), 20.5 (CH_3, C-6′); ESMS *m/z* 491.1 $[M + H]^+$ and 513.0 $[M + Na]^+$; HRESIMS *m/z* 491.1630 $[M + H]^+$ (calcd for $C_{21}H_{32}ClN_2O_7S$, 491.1619).

Compound 19: colorless gum; UV (CH_3CN/H_2O) λ_{max} 230 (sh) nm; ^1H NMR (DMSO-d_6) δ 9.02 (1H, brs, NH), 8.39 (1H, d, $J = 8.0$ Hz, NH), 5.79 (1H, m, H-7), 5.72 (1H, m, H-8), 5.52 (1H, d, $J = 8.0$ Hz, OH), 4.43 (1H, m, H-2′), 3.67 (1H, m, H-5), 3.65 (2H, m, H_2-13), 3.63 (3H, s, CO_2Me), 2.76 (2H, m, H_2-1′), 2.61 (1H, t, $J = 8.0$ Hz, H-2), 2.28 (1H, m, H-6), 1.90 (2H, m, H_2-12), 1.85 (3H, s, H_3-6′), 1.78 (2H, m, H_2-9), 1.75 (1H, m, H-11a), 1.72 (3H, s, H_3-14), 1.70 (1H, m, H-10a), 1.40 (1H, m, H-10b), 1.21 (1H, m, H-11b); ESMS *m/z* 455 $[M + H]^+$; HRESIMS *m/z* 455.1866 $[M + H]^+$ (calcd for $C_{21}H_{31}N_2O_7S$, 455.1852).

***In Vitro* Purified Rabbit Muscle 20S CT-L Proteasome Assay.** The CT-L activity of the 20S proteasome was measured as described previously[21,22] with some minor modifications. Briefly, serially diluted compounds were added in duplicate to 1 μg/mL purified rabbit 20S proteasome in assay buffer containing 20 mM HEPES, pH 7.3, 0.5 mM EDTA, 0.05% Triton X-100, and 0.035% SDS and preincubated for 5 min at 37 °C. Reactions were initiated by the addition of the Suc-LLVY-AMC peptide substrate at a final concentration of 20 μM. Fluorescence of the cleaved peptide substrate was measured at λ_{ex} = 390 nm and λ_{em} = 460 nm using a Fluoroskan Ascent 96-well microplate reader (Thermo Electron, Waltham, MA). The IC_{50} values (the drug concentration at which 50% of the maximal relative fluorescence is inhibited) were calculated by Prism (GraphPad Software) using a sigmoidal dose−response, variable slope model. IC_{50} values of at least three independent experiments are represented as the mean ± standard deviation.

Growth Inhibition Assays. RPMI 8226 cells were plated at a density of 2×10^4 cells/well in 96-well plates. Serially diluted compounds were added in triplicate, and the cells were incubated for 48 h. Cell growth was assessed by measuring the reduction of resazurin with a fluorometer (Perkin-Elmer, Torrance, CA). The IC_{50} values (the drug concentration at which 50% of the maximal observed growth inhibition is established) were determined using a standard sigmodial dose−response curve fitting algorithm, XLfit 3.0 (ID Business Solutions Inc., Alameda, CA).

Acknowledgment. We gratefully acknowledge W. Fenical and P. Jensen of Scripps Institution of Oceanography for their pioneering work in the discovery of *Salinispora tropica* and salinosporamide A, and for providing the original, authentic standards of **3** and **4**. We thank A. Rheingold, University of California, San Diego, and S. Kassel, Villanova University, for determining the X-ray crystal structure of **9** and for their expert advice. We also thank B. Mai for acquiring HRMS data on a number of the analogues.

Supporting Information Available: ^1H NMR spectra for new compounds. This material is available free of charge via the Internet at http://pubs.acs.org.

References and Notes

(1) Adams J. *Proteasome Inhibitors in Cancer Therapy*; Humana Press: Totowa, NJ, 2004.
(2) Groll, M.; Huber, R. *Biochem. Biophys. Acta* **2004**, *1695*, 33−34.
(3) Koguchi, Y.; Kohno, J.; Nishio, M.; Takahashi, K.; Okuda, T.; Ohnuki, T.; Komatsubara, S. *J. Antibiot.* **2000**, *53*, 105−109.
(4) Asai, A.; Hasegawa, A.; Ochiai, K.; Yamashita, Y.; Mizukami, T. *J. Antibiot.* **2000**, *53*, 81−83.
(5) Hanada, M.; Sugawara, K.; Kaneta, K.; Toda, S.; Nishiyama, Y.; Tomita, K.; Yamamoto, H.; Konishi, M.; Oki, T. *J. Antibiot.* **1992**, *45*, 1746−1752.
(6) Fenteany, G.; Standaert, R. F.; Reichard, G. A.; Corey, E. J.; Schreiber, S. L. *Proc. Natl. Acad. Sci.* **1994**, *91*, 3358−3362.
(7) Omura, S.; Fujimoto, T.; Otoguro, K.; Matsuzaki, K.; Moriguchi, R.; Tanaka, H.; Sasaki, Y. *J. Antibiot.* **1991**, *44*, 113−116.
(8) Omura, S.; Matsuzaki, K.; Fujimoto, T.; Kosuge, K.; Furuya, T.; Fujita, S.; Nakagawa, A. *J. Antibiot.* **1991**, *44*, 117−118.
(9) Feling, R. H.; Buchanan, G. O.; Mincer, T. J.; Kauffman, C. A.; Jensen, P. R.; Fenical, W. F. *Angew. Chem., Int. Ed.* **2003**, *42*, 355−357.
(10) Williams, P. G.; Buchanan, G. O.; Feling, R. H.; Kauffman, C. A.; Jensen, P. R., Fenical, W. *J. Org. Chem.* **2005**, *70*, 6196−6203.
(11) Maldonado, L. A.; Fenical, W.; Jensen, P. R.; Kauffman, C. A.; Mincer, T. J.; Ward, A. C.; Bull, A. T.; Goodfellow, M. *Int. J. Syst. Evol. Microbiol.* **2005**, *55*, 1759−1766.
(12) Stadler, M.; Seip, S.; Muller, H.; Mayer-Bartschmid, A.; Bruning, M.; Benet-Buchholz, J.; Togame, H.; Dodo, R.; Reinemer, P.; Bacon, K.; Fuchikami, K.; Matsukawa, S.; Urbahns, K. International Patent, WO 2004/071382 A2, 2004.
(13) Macherla, V. R.; Mitchell, S. S.; Manam, R. R.; Reed, K. A.; Chao, T.; Nicholson, B.; Deyanat-Yazdi, G.; Mai, B.; Jensen, P. R.; Fenical, W. F.; Neuteboom, S. T. C.; Lam, K. S.; Palladino, M. A.; Potts, B. C. M. *J. Med. Chem.* **2005**, *48*, 3684−3687.
(14) Groll, M.; Huber, R.; Potts, B. C. M. *J. Am. Chem. Soc.* **2006**, *128*, 5136−5141.
(15) Dick, L. R.; Cruikshank, A. A.; Grenier, L.; Melandri, F. D.; Nunes, S. L.; Stein, R. L. *J. Biol. Chem.* **1996**, *271*, 7273−7276.
(16) Dick, L. R.; Cruikshank, A. A.; Destree, A. T.; Grenier, L.; McCormack, T. A.; Melandri, F. D.; Nunes, S. L.; Palombello, V. J.; Parent, L. A.; Plamondon, L.; Stein, R. L. *J. Biol. Chem.* **1997**, *272*, 182−188.
(17) Groll, M.; Ditzel, L.; Lowe, J.; Stock, D.; Bochtler, M.; Bartunik, H. D.; Huber, R. *Nature* **1997**, *386*, 463−471.
(18) Lam, K. S.; Tsueng, G.; McArthur K. A.; Mitchell, S. S.; Potts, B. C. M.; Xu, J. *J. Antibiot.*, in press.
(19) Pretsch, E.; Seible, J.; Simon, W.; Clerc, T. *Tables of Spectral Data for Structure Determination of Organic Compounds*; Springer-Verlag: Berlin, 1989; p C46,
(20) Jensen, P. R.; Dwight, R.; Fenical, W. *Appl Environ. Microbiol.* **1991**, *57*, 1102−1108.
(21) Stein, R. L.; Melandri, F.; Dick, L. *Biochemistry* **1996**, *35*, 3899−3908.
(22) Lightcap, E. S.; McCormack, T. A.; Pien, C. S.; Chau, V.; Adams, J.; Elliott, P. J. *Clin. Chem.* **2000**, *46*, 673−683.

NP0603471